

**Direct readout Meteorological Satellite Data Processing with a
Low-Cost, Computer-Linked System**

By
T.H. Vonder Haar, D. Reynolds and L. Lilie

Department of Atmospheric Science
Colorado State University
Fort Collins, Colorado

September 1974



**Department of
Atmospheric Science**

Paper No. 227

DIRECT READOUT METEOROLOGICAL SATELLITE DATA PROCESSING
WITH A LOW-COST, COMPUTER-LINKED SYSTEM

by

T. H. Vonder Haar

D. Reynolds

L. Lilie

Department of Atmospheric Science

Colorado State University

Fort Collins, Colorado

September, 1974

Atmospheric Science Paper No. 227

ABSTRACT

Visible and infrared image data from the scanning radiometer on the NOAA-2 and NOAA-3 satellites are received by a VHF "APT" Station at Colorado State University. In addition to producing the regular hard-copy photographs, the taped signal is specially processed by electronic means, converted from analog to digital form and further processed in the computer. Details of the processing steps and equipment will be described and the meteorological application of the full-resolution processed images will be noted for cases of both synoptic and mesoscale weather situations.

LIST OF FIGURES

- Figure 1 Flow chart of satellite signal reception, digitization analysis and quantitative data output.
- Figure 2 The NOAA-3 polar-orbiting satellite which provides direct-readout visible and infrared information which is received at the CSU satellite ground station (10 db gain antenna, VHF receiver, stereo tape deck and antenna driver, and Muirhead photofacsimile).
- Figure 3 a) Discriminator box designed and built at Colorado State University; b) Video output signal from the discriminator box showing visible portion of the earth scan, space scan, step-wedge, satellite housing and IR space scan. A blow-up of the step-wedge is also provided.
- Figure 4 Computer output from program TAPE DUMP which locates the step-wedge in the set of 25 lines and also shows that the data is acceptable.
- Figure 5 Computer output from the program LOW RESOLUTION where Colorado is outlined. This output provides display of the entire horizon-to-horizon scan in which the data has been averaged.
- Figure 6 Example of the visible and infrared SR data from the NOAA satellites as output by a Muirhead photofacsimile for March 18, 1974. Note orographic clouds in south central and south-eastern Colorado. Visible image is on left; infrared on right.

LIST OF FIGURES (cont.)

- Figure 7 High resolution digitized and mapped infrared data for March 18, 1974 where orographic clouds are outlined. Only temperatures between 225°K and 250°K are displayed (A= 225°K , B= 226°K , etc.).
- Figure 8 Rawinsonde plot taken at Durango, Colorado at 1205 MDT showing a well-defined orographic cloud between 592-515 mb while another deck of clouds occurred above 450 mb as noted by observer.
- Figure 9 Hard copy print of the SR data (IR, left; visible, right) showing well-developed "upslope" system in eastern Wyoming and Colorado. IR picture shows some active convection taking place within the general cloud band.
- Figure 10 Radar summary provided by the National Weather Service for 1740Z (1140 MDT) for 19 July, 1973 showing that one large thunderstorm was in existence in extreme eastern Colorado with a top to 39,000 ft.
- Figure 11 Computer output from the HIGH RESOLUTION PROGRAM where the borders of Colorado are outlined. Temperature representation as given by each letter is provided on the right. Blank area in eastern Colorado is temperature below 240°K .
- Figure 12 Rawinsonde plot of the Grover, Colorado sounding taken on July 19, 1973 at 1100 MDT. Plot shows a very moist low to middle atmosphere with strong upslope motion in the lower levels.

LIST OF FIGURES (cont.)

- Figure 13 High Resolution (IR) output where only the higher type clouds have been depicted. Data displayed in this way can help define the areal extent of the high clouds as well as pin-point their location.
- Figure 14 Visible (left) and IR (right) NOAA SR data for March 10, 1974 showing an upslope snowstorm system over eastern Colorado and northern New Mexico. Note contrast between the visible and IR data.
- Figure 15 High resolution (IR) output for March 10, 1974 where areas within the black line have temperatures above 252°K . Those colder than 252°K are areas where the heavier precipitation would be most likely to occur.
- Figure 16 Schematic electrical diagram of the "Discriminator Box" used in the digitizing of the NOAA SR data.

TABLE OF CONTENTS

	<u>page</u>
ABSTRACT.	i
LIST OF FIGURES	ii
TABLE OF CONTENTS	v
1.0 INTRODUCTION	1
2.0 BASIC SYSTEMS COMPONENTS	2
2.1 Satellite Tracking and Signal Reception	2
2.2 Satellite Signal Processing	5
2.3 Analog-to-Digital Conversion.	7
2.4 Computer Processing and Display	7
3.0 EXAMPLES OF APPLICATION OF QUANTITATIVE DATA	13
4.0 SUMMARY.	26
5.0 REFERENCES	29
6.0 ACKNOWLEDGEMENTS	30
Appendix 1.	31
Appendix 2.	38

1.0 INTRODUCTION

The first direct-readout Automatic Picture Transmission (APT) of visual image data from Vidicon sensors was inaugurated by an experiment on TIROS-7 (1963). A second direct-readout milestone occurred in the late 1960's when the Direct Readout Infrared Radiometer (DRIR) on Nimbus-3 (1969) and others on USSR satellites allowed local users to acquire both daytime and nighttime data. A third advance took place in 1970-71 when the Scanning Radiometer (SR) experiment on ITOS-1 allowed reception of simultaneous visual and infrared data (during daytime). (For details of this experiment see Schwalb, 1972).

The purpose of the present paper is to describe and demonstrate the fourth advance in VHF direct-readout meteorological satellite data reception. It is the capability to locally digitize and computer-process the SR data in quantitative form, thus expanding its usefulness for both research and operational applications. This new opportunity for direct readout users is made possible by the relatively low cost and high performance of present-day electronics components and of small computer systems.

After the calibrated infrared data became available, Myers et al., (1970) described a method to work with gray-wedge data using analog methods. Shortly thereafter Miller and Vonder Haar (1972) demonstrated that digitized SR and (and APT) data could provide the bi-spectral view to local users that had such value as noted by Vonder Haar (1970). Miller and Vonder Haar (1972) described a first modification to a local "APT" station that could produce digitized data. The present paper discusses an improved station in existence in the Department of Atmospheric

Science, Colorado State University (CSU), Fort Collins, Colorado. It also presents application examples of the digitized direct-readout SR data from the NOAA-2 and NOAA-3 satellites.

The applications of the direct readout meteorological satellite data fall into several categories. For example, weather forecasting units can use these data in various forecasting operations. In addition, real-time support for scientific field experiments is becoming an important area of application. Even for research after-the-fact the full resolution data are often most accessible to scientists from direct readout ground units since the large data archives may contain only processed and averaged data.

2.0 BASIC SYSTEM COMPONENTS

The components of the CSU system are displayed in Figure 1; some equipment is shown in Figure 2. The flow-chart denotes the four main steps in the satellites data processing:

- 1) Reception and recording of the VHF signal;
- 2) Discrimination of the signal components;
- 3) Analog-to-digital processing; and
- 4) Computer processing and display.

2.1 Satellite Tracking and Signal Reception

Satellite tracking information and VHF signal reception has been well documented (NESC, 1969; Vermillion, 1969) and will not be discussed here. We use computer generated tracking information rather than that

**CHART OF SATELLITE DIRECT READOUT AND SIGNAL
PROCESSING**

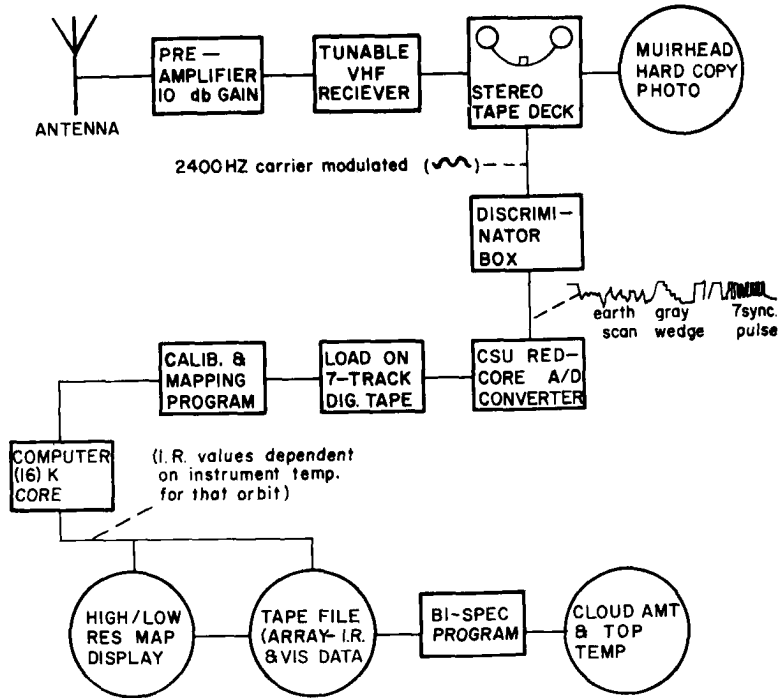


Figure 1 Flow chart of satellite signal reception, digitization analysis and quantitative data output.

NOAA-3

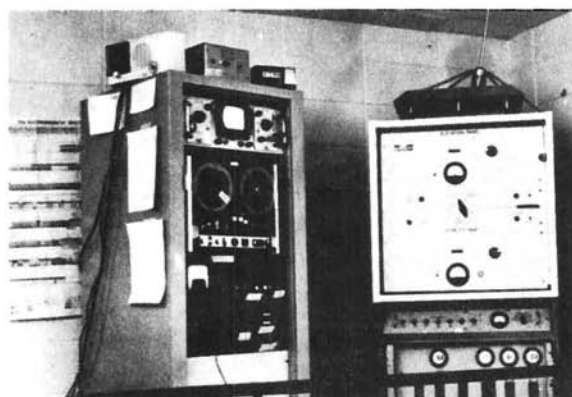
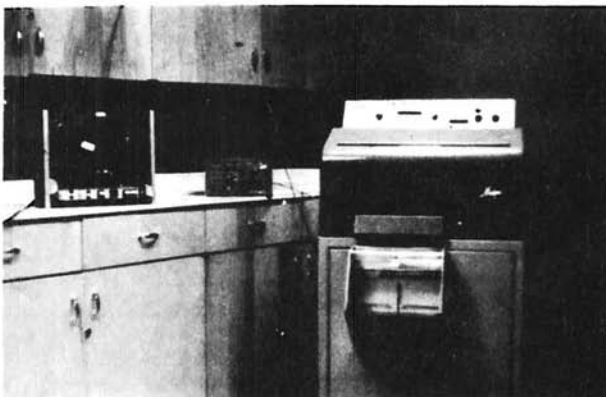
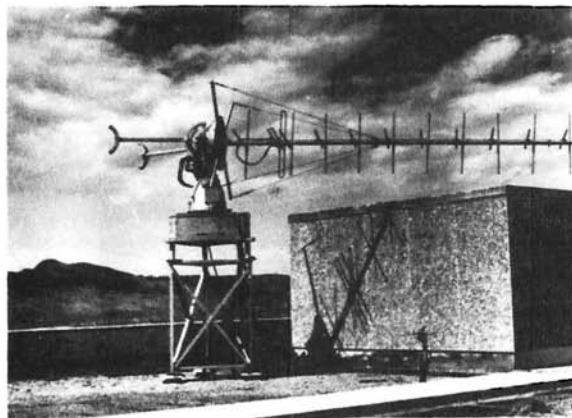
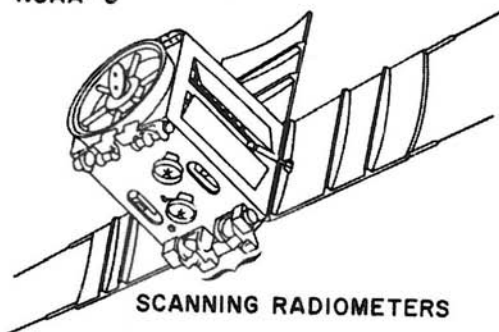


Figure 2 The NOAA-3 polar-orbiting satellite which provides direct-readout visible and infrared information which is received at the CSU satellite ground station (10db gain antenna, VHF receiver, stereo tape deck and antenna driver, and Muirhead photofacsimile).

obtained from a plotting board. As noted in Figs. 1 and 2, secondary output from the quantitative signal processing flow are the hardcopy photographs of the SR images as produced on a standard Muirhead photo-facsimile system.

2.2 Satellite Signal Processing

After tape recording the 2400 Hz carrier which is amplitude-modulated by the video (see Schwalb, 1972) the signal is processed by a specially built electronics unit. This unit, termed the "discriminator box" is designed to facilitate subsequent digitizing and has a twofold purpose:

- a) to convert the amplitude modulated carrier into an analog video signal; and
- b) to locate the synchronization pulses as they occur in the video signal.

A small photo of the discriminator box is shown in Figure 3a. Figure 3b displays the output from the box as noted in (a) above. The actual signal, from a NOAA satellite reception, shows the sync pulses, typical video, and the calibration wedge which is also digitized and used in the subsequent computer processing. In practice the location of sync pulses by the discriminator box is not strictly necessary since it could be done in the computer. However, the reduced expense and more sophisticated means to do it electronically makes the rather inexpensive (\$300 for material) discriminator box the most attractive option. Details of the construction and operation of the discriminator box are provided in Appendix 1.

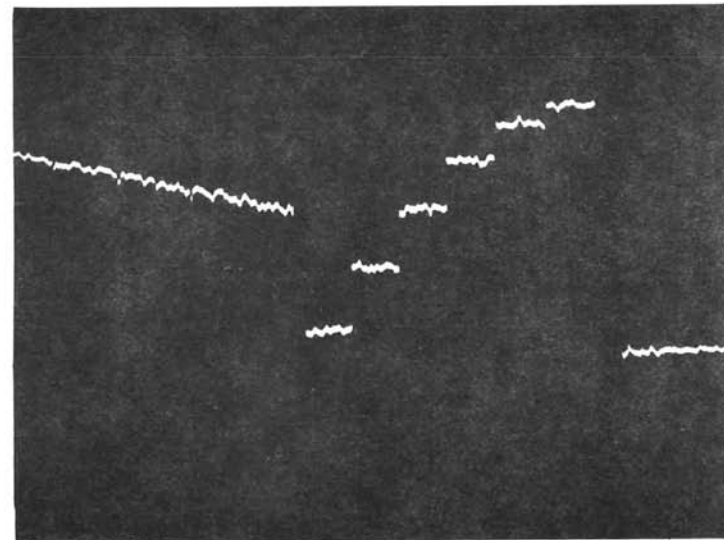
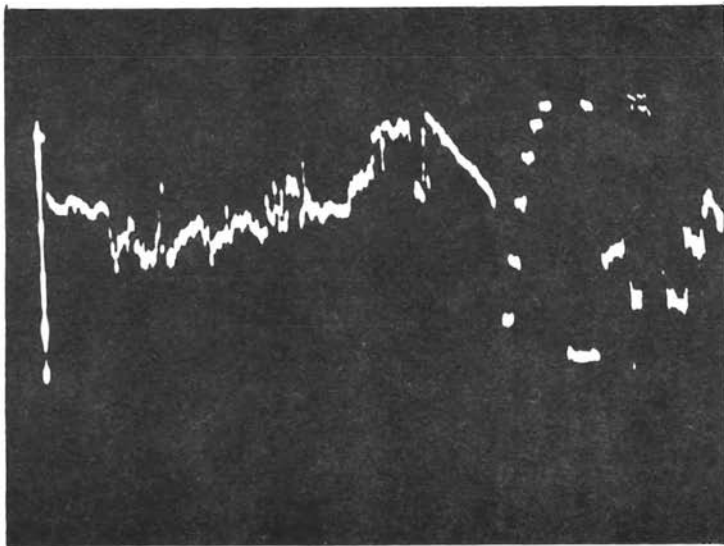
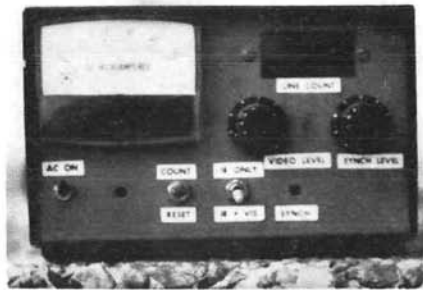


Figure 3 a) Discriminator box designed and built at Colorado State University; b) Video output signal from the discriminator box showing visible portion of the earth scan, space scan, step-wedge, satellite housing and IR space scan. A blow-up of the step-wedge is also provided.

2.3 Analog-to-Digital Conversion

Digitizing NOAA's Scanning Radiometer data without loss of nominal ground resolution (~4 n. mi.) requires a real-time sampling rate of ~1000 samples per second. This is well within the capability of a wide range of small A/D systems of which we use a REDCOR system available at Colorado State University. Only a single channel input is required. The detected synchronization pulse is used to start the digitizing process such that one digital record on 7-track magnetic tape corresponds to a single satellite video scan line. The infrared and visual light portions of each video record may be separated at the discriminator box or during computer processing.

2.4 Computer Processing and Display

After digitizing the satellite video is in the form of digital counts ranging from 0.0 - 4,096 arranged in a scan-line, picture element coordinate system. The data then must be processed through four separate software programs which are:

- 1) Tape dump;
- 2) Calibration;
- 3) Low resolution; and
- 4) High resolution

Programs (1) and (2) are necessary for converting the data from digital volts to satellite volts. Programs (3) and (4) are used to:

- a) Convert either from satellite volts to reflectance values for the visible, or blackbody temperature for the IR; and
- b) Display these values in gridded form.

Other programs could be developed depending on the complexity of the analysis and display desired. Specifically, the function of each program is:

TAPE DUMP

Gives a visual display of the data to: (see Fig. 4)

- a) check the quality of the data; and
- b) to locate the position of the calibration wedge in the visible portion of the SR data.

Figure 9 shows the wedge on the visible picture. Out of 25 scan lines only 14 have the step wedge information. It is these 14 lines which must be located, which in turn determines the start time of the data, this location then being used as input into the calibration program. If the step-wedge cannot be found in a set of 25 lines, the data is dropped.

The TAPE DUMP program not only determines the location of the step-wedge in the set of 25 lines, but also calculates the total number of scan lines (computer records). These two values are then input to the calibration program.

CALIBRATION PROGRAM

The purpose of the CALIBRATION PROGRAM is to linearize the digitized step-wedge to the pre-launch voltages (see Appendix II) determined for each wedge using the least-squares method. Thus this allows conversion from digitized computer volts to satellite volts. An averaging scheme is used to try to account for changes in the step-wedge during one satellite pass. The data is broken down into 10 groups of 25 lines each. For the visible this would be the first 10 groups of 25 lines where those 25 lines contain 14 with step-wedge information. For the IR it would be

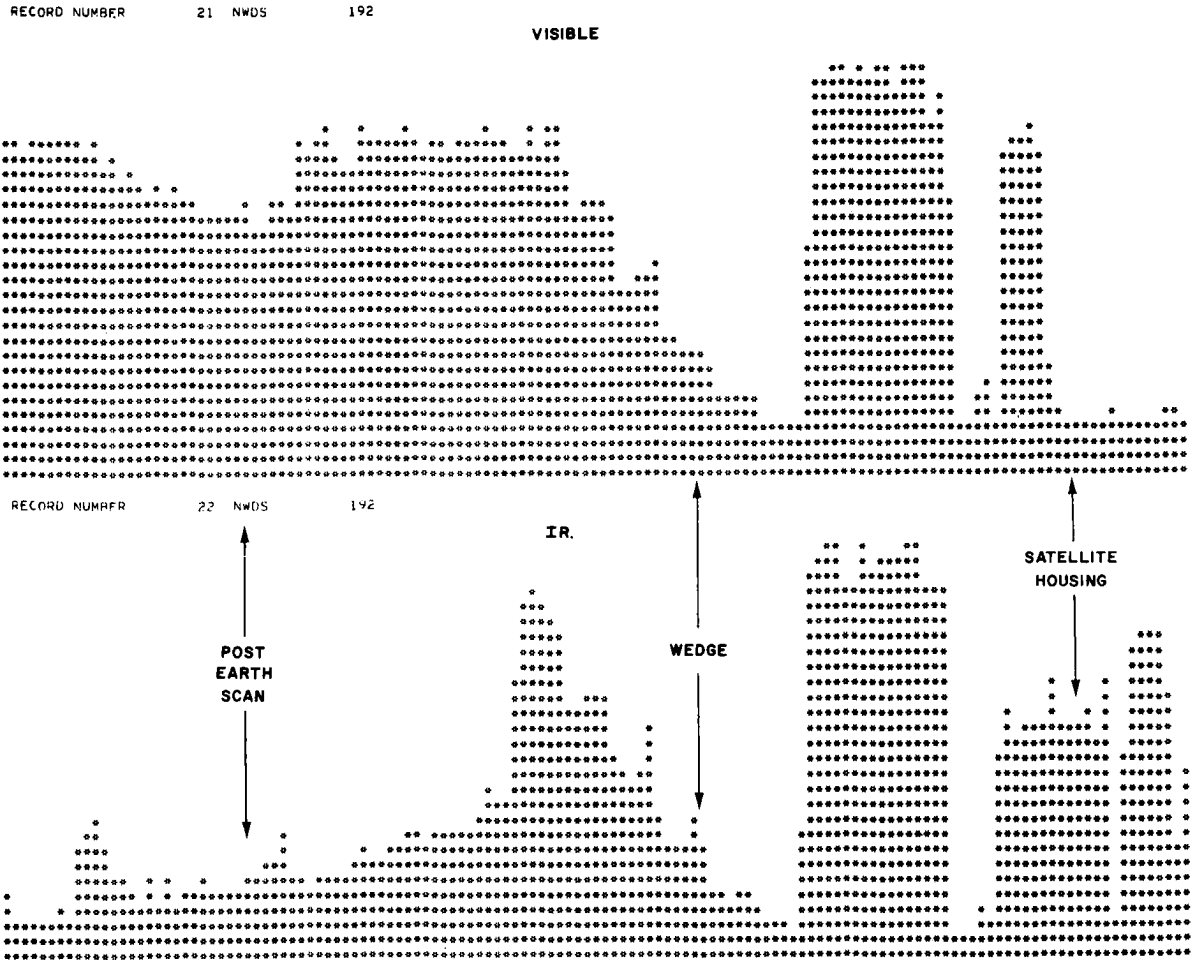


Figure 4 Computer output from program TAPE DUMP which locates the step-wedge in the set of 25 lines and also shows that the data is acceptable.

10 groups of 25 lines which all contain step-wedge information. Coefficients for this set of data are determined and applied to the first 275 lines of data. New coefficients are then calculated for each successive set of 25 lines by averaging the prior 10 groups of 25 lines for the rest of the data. The coefficients are then punched on cards to be used in the LOW and HIGH RESOLUTION PROGRAMS.

LOW RESOLUTION PROGRAM

Once the conversion from computer volts to satellite volts has been made the data can be converted either to brightness values (and then to short-wave radiances) or blackbody temperatures for the IR once the housing temperature of the satellite during that orbit is known. The relationship between satellite volts and brightness or blackbody temperature as a function of satellite housing temperature is provided by the National Environmental Satellite Service (NESS) from pre-launch calibrations (see Appendix II). The housing temperature for each orbit may be obtained from the Operations Section of NESS. The conversion takes place in the LOW RESOLUTION PROGRAM. The input needed to this program is:

- 1) satellite tracking information (from TBUS bulletin) which allows location and mapping of the data;
- 2) the calibration cards from the calibration program;
- 3) the satellite housing temperature coefficient cards as given in Appendix II for the visible data;
- 4) satellite orbit number, start time of the data to initialize mapping (for details of mapping and listings of other programs see Madden et al., 1972 and Madden and Parsons, 1973); and
- 5) coefficients of the 4th degree polynomial derived by a least-squares fit of satellite volts vs. IR temperature for a given housing temperature (Appendix II).

The output from the LOW RESOLUTION PROGRAM is a gridded array (2° latitude by 5° longitude) of SR data (visible or IR) which has been averaged by taking every 5.5 data points in the east-west direction and every 2 data points in the north-south direction and deriving one number which is displayed. This gives 120 data points across normal computer paper (see Fig. 5). An alphanumeric character display is given in low resolution where $A=1-2 \text{ watts/m}^2$, $B=3-4 \text{ watts/m}^2$, etc. for visible, while $200^{\circ}\text{K} < A < 205$, $205 < B < 210^{\circ}\text{K}$, etc., for the IR data. These intervals are chosen at will and can be whatever one desires. The only limit is the number of different characters capable of being printed by the computer. Once the low resolution display is output it can be checked for earth location by using the hard-copy photograph provided by the Muirhead Mufax and checking known landmarks and cloud locations of these landmarks with the locations of the clouds on the mapped low resolution display. Also areas where further study is desired can be located for blow-up in the high-resolution program.

HIGH RESOLUTION PROGRAM

The HIGH RESOLUTION PROGRAM displays the visible and IR data for each data point on a 1° latitude by 1° longitude grid. Thus the full-resolution data (4 n. mi. at sub-satellite point) is available for examination from this program. The input parameters are the same as for the low-resolution except location parameters (x, y location given by number of data points into a record and time of record) for the area of interest are also necessary. Again an alphanumeric character display is available and any range of data can be displayed as will be shown in section 3.0.

3.0 EXAMPLES OF APPLICATION OF QUANTITATIVE DATA

The final output of the direct readout data processing described above is an earth-located array of data on computer tape for both the infrared and visible images. With the data in this form it is possible to statistically analyze the data by latitude and longitude (Sikula and Vonder Haar, 1974) or quantitatively compare and determine relationships between the visible and infrared data which is available simultaneously at each point (Bi-Spec; Vonder Haar and Reynolds, 1974).

Some examples of the way in which the quantitative data has been used are:

1) Opportunity recognition in weather modification experiments.

In the seeding of cold orographic clouds it has been found that with cloud-top temperatures within a certain specific range (-10 to -25°C), seeding has much more beneficial results than with seeding outside this range (Grant and Elliott, 1974). Since the SR data contains infrared information in the atmospheric window ($10.5 - 12.5\mu\text{m}$) it is possible with the quantitative data to determine the "skin" temperature of the cloud top and thus determine if seeding of that cloud would be beneficial. Fig. 6 is the hard copy photograph of March 18, 1974 showing a well-developed orographic cloud situated over the San Juan Mountains in extreme south-central Colorado. The Bureau of Reclamation is conducting a pilot seeding project over the San Juan's during the winter months, so a preliminary study was conducted to determine whether satellite data could aid in their decision making. A high resolution display of this area for the infrared is shown in Fig. 7 with temperatures between the range of $225-250^{\circ}\text{K}$ characterized (A= 225°K , B= 226°K , etc.; all temperatures greater than 250°K or less than

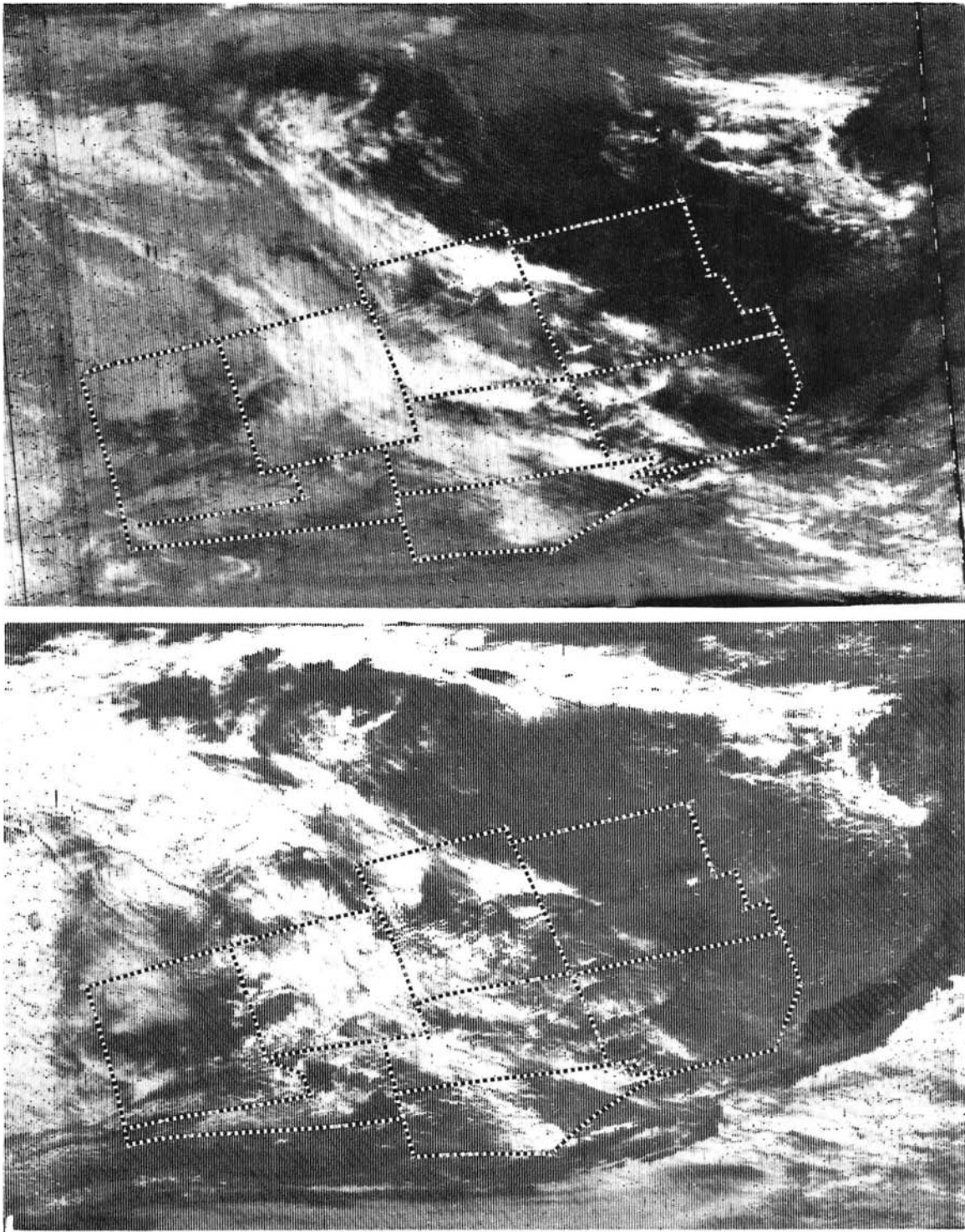


Figure 6 Example of the visible and infrared SR data from the NOAA satellites as output by a Muirhead photofacsimile for March 18, 1974. Note orographic clouds in south central and south-eastern Colorado. Visible image is on left; infrared on right.

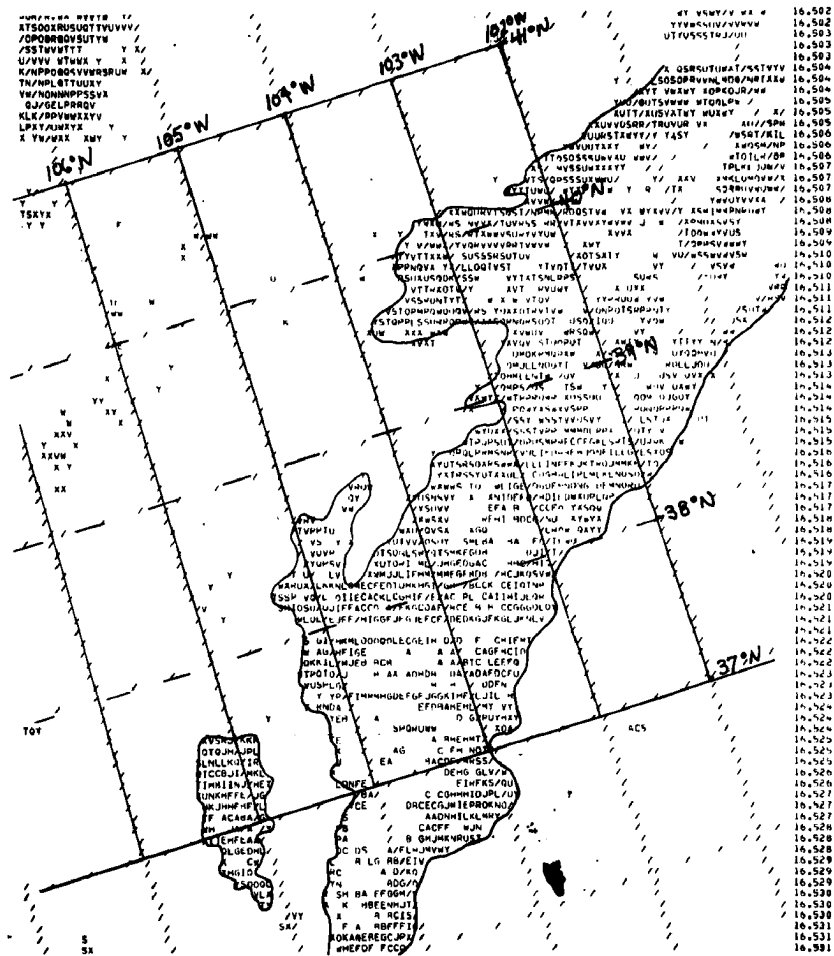


Figure 7 High resolution digitized and mapped infrared data for March 18, 1974 where orographic clouds are outlined. Only temperatures between 225°K and 250°K are displayed (A=225°K, B=226°K, etc.).

225°K have been blanked). Here we can see that the orographic cloud at 37°N, 106°W has a top temperature somewhere between -30 and -40 which is too cold for seeding. However, this one case points out one precaution that must be observed in using only the satellite data. In this case there were two decks of clouds as can be seen from the sounding taken at Durango, Colorado at 1205 MDT, 1½ hrs. after the satellite pass (Fig. 8). One deck of clouds was the orographic cloud located between 600 mb and 500 mb (with a top temperature in the "seed" range), while another deck of higher clouds was between 450 mb and 300 mb which is what the satellite was seeing. Thus it is necessary to have not only the digitized satellite data but also to have some additional observations to correlate with. However, as can be seen from Fig. 6, there could be no better way of describing and obtaining mean cloud temperatures for a large area such as the San Juan Mountains.

2) As a forecast aid to predicting heavy "upslope" type rain (flash floods) along the front range and high plains regions of the Rocky Mountains.

Fig. 9 is the hard copy print of 19 July, 1973. Qualitatively these pictures show extensive cloudiness in the northern half of Colorado and almost all of Wyoming. The brightest clouds appearing in the visible picture also appear to be the coldest or whitest in the IR picture thus suggesting these clouds are the deepest and probably the precipitating areas. The radar summary (Figs. 10) taken approximately one hour after the satellite pass shows the largest cell in the general upslope cloudiness in extreme eastern Colorado topping out at 37,000 feet. This corresponds to the large white cloud on the IR picture located in this same area. Thus qualitatively we have been able to define some convective

USAF SKEW T, log p DIAGRAM

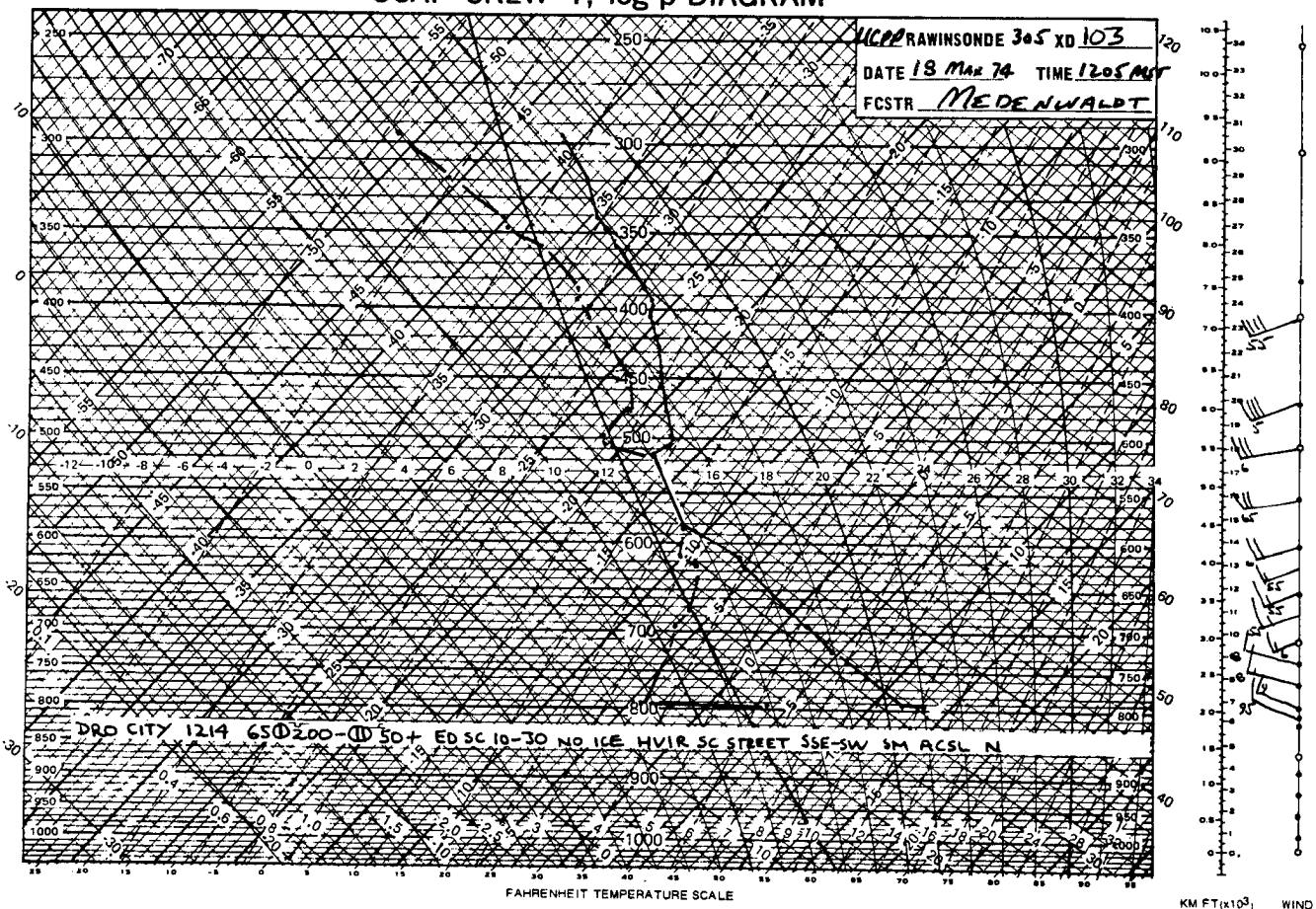


Figure 8 Rawinsonde plot taken at Durango, Colorado at 1205 MDT showing a well-defined orographic cloud between 592-515 mb while another deck of clouds occurred above 450 mb as noted by observer.

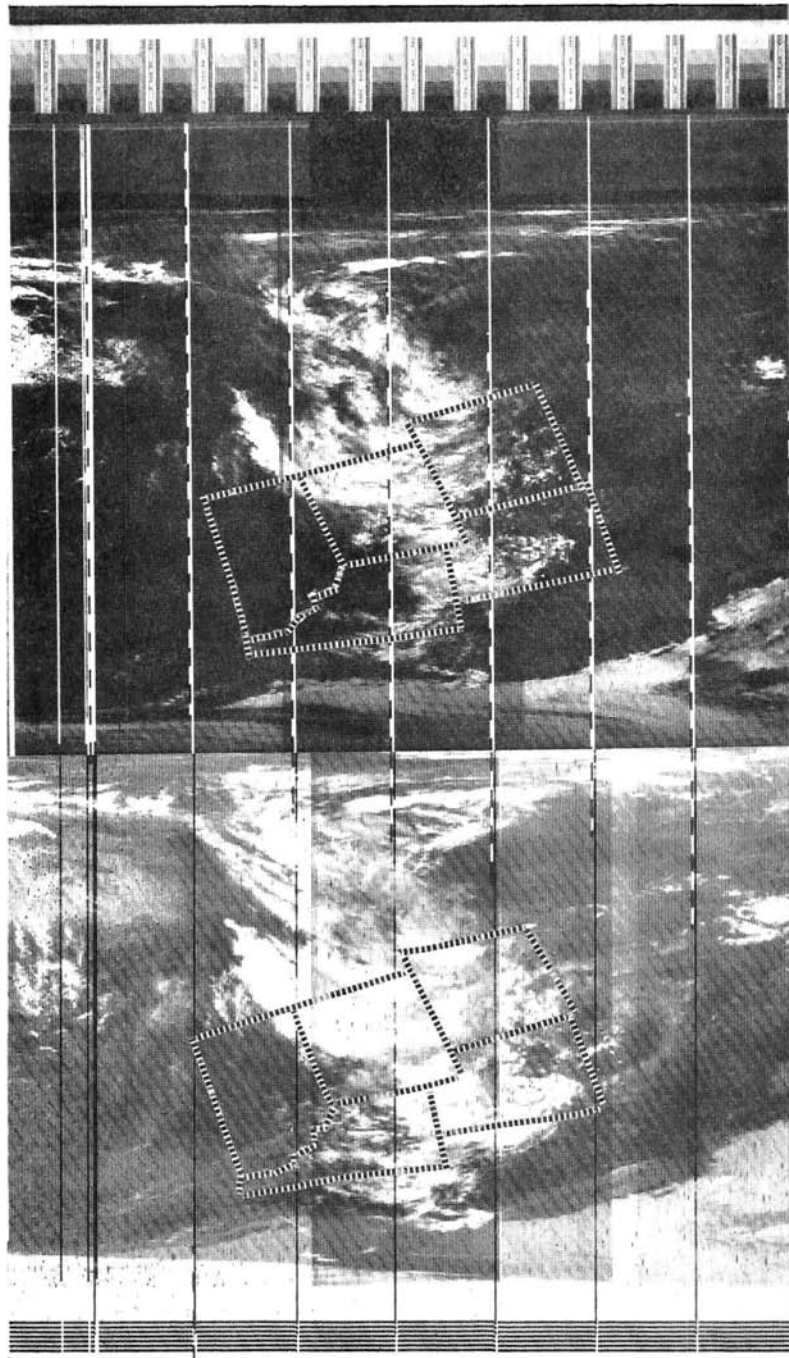


Figure 9 Hard copy print of the SR data (IR, left; visible, right) showing well-developed "upslope" system in eastern Wyoming and Colorado. IR picture shows some active convection taking place within the general cloud band.

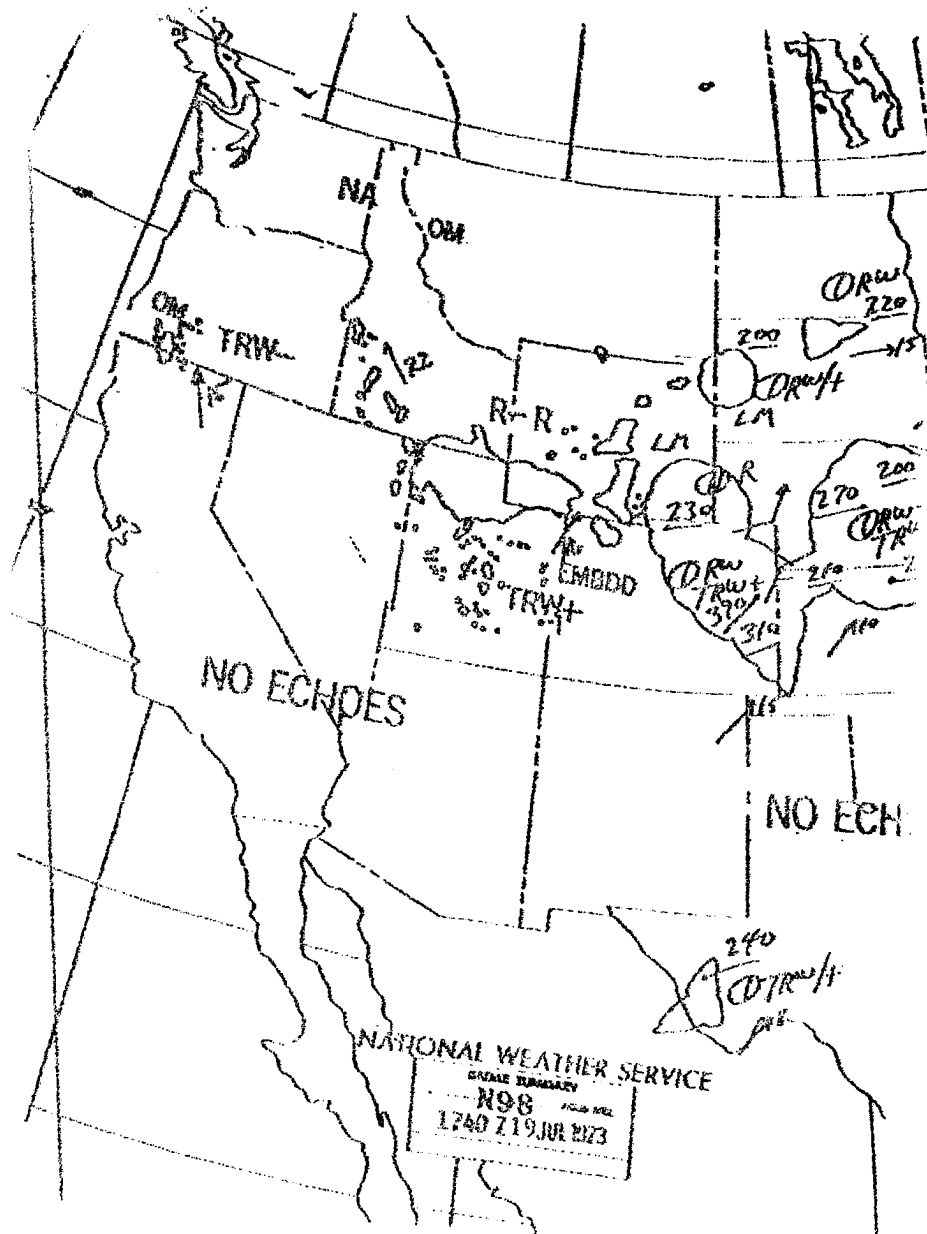
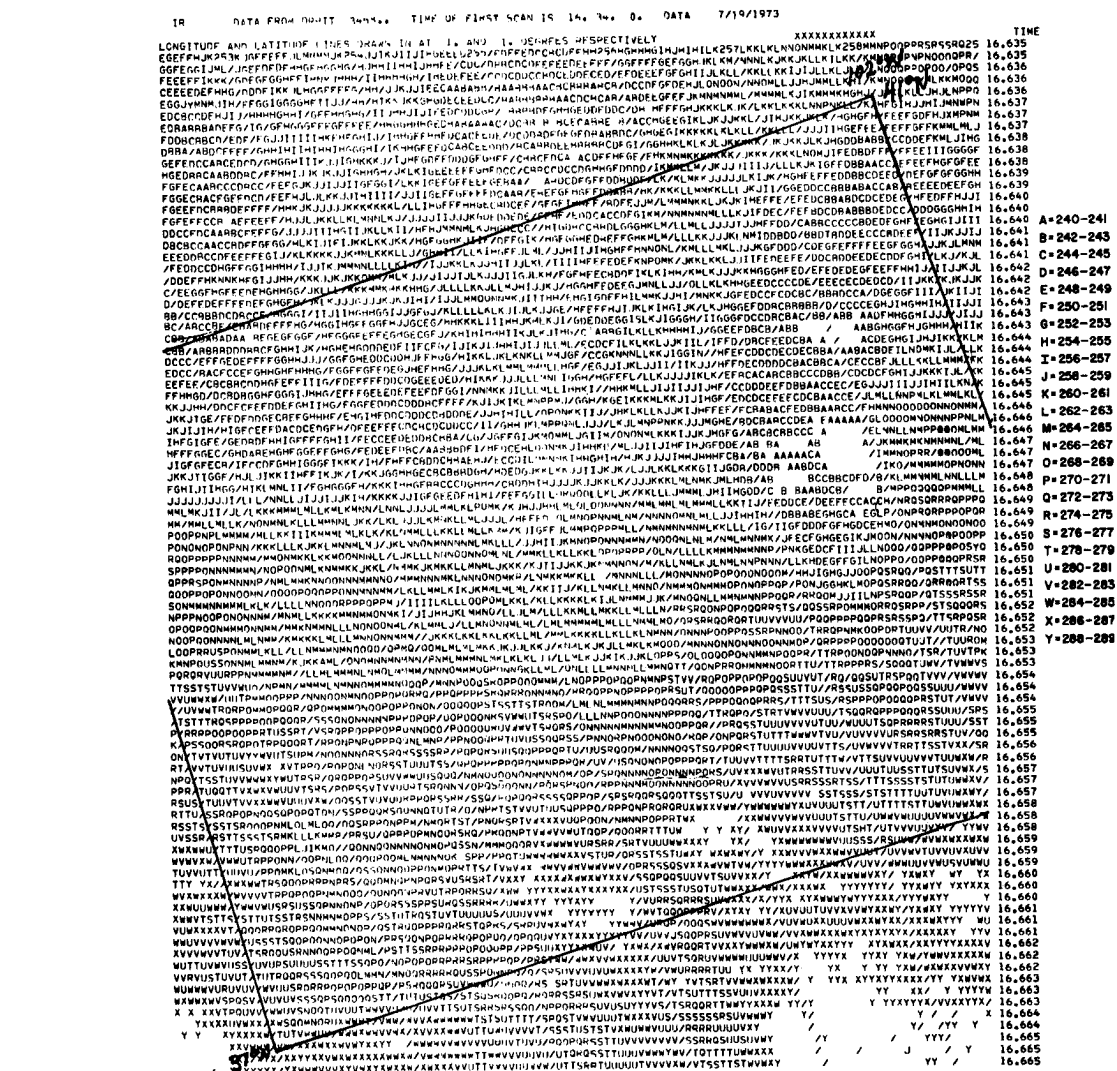


Figure 10 Radar summary provided by the National Weather Service for 1740Z (1140 MDT) for 19 July, 1973 showing that one large thunderstorm was in existence in extreme eastern Colorado with a top to 39,000 ft.

cells imbedded in a general upslope storm system. This is one clue that heavy rains may be possible, and over a very large area. Quantitatively Fig. 11, a high resolution display of the area, allows one to define the general cloud top of the upslope cloudiness along with identifying the larger convective cells. The IR data shows that most of the general upslope clouds have tops between $250 - 260^{\circ}\text{K}$ or -13 to -23°C . The large convective clouds are shown by areas of A's, B's, C's and in one case a large blank area where the top temperature is below 240°K . Since we have now obtained the general cloud top temperatures and areal extent and location it is possible to obtain heights of the clouds using radiosonde information. A sounding was taken at 1100 MDT at Grover, Colorado (110 mi. NNE of Denver) in cooperation with the National Hail Research Experiment (NHRE) (Fig. 12). The sounding immediately shows the very moist low levels along with a strong easterly (upslope) component low level wind into the mountains. Also good speed and directional wind shear aloft is dynamically driving the storm system. The sounding thus aides in the forecasting of a possible heavy rain situation but this is only a spot sample. The satellite data shows that these conditions probably exist on the synoptic scale. In relation to cloud heights the sounding shows that the -13°C to -23°C temperature range is between 450 and 350 mb or between 20,000 and 27,000 feet. This agrees with what radar was seeing during the storm. The higher, deeper convection, shown in Fig. 13, where the lower clouds have been blanked, have top temperatures at 235°K or somewhat below as seen by the blank area in the cloud at 39°N , 103°W . A temperature of -40°C would put the top up near 200 mb or 38,000 feet. This again agrees



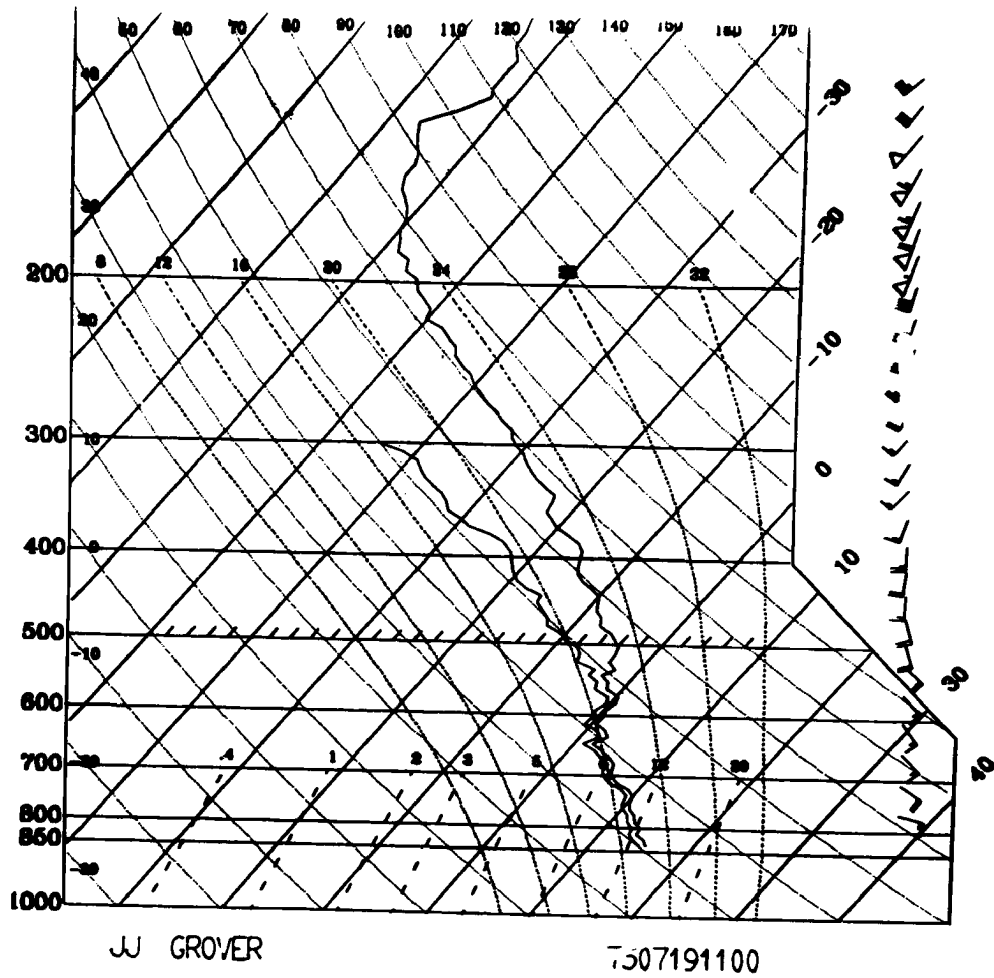


Figure 12 Rawinsonde plot of the Grover, Colorado sounding taken on July 19, 1973 at 1100 MDT. Plot shows a very moist low to middle atmosphere with strong upslope motion in the lower levels.

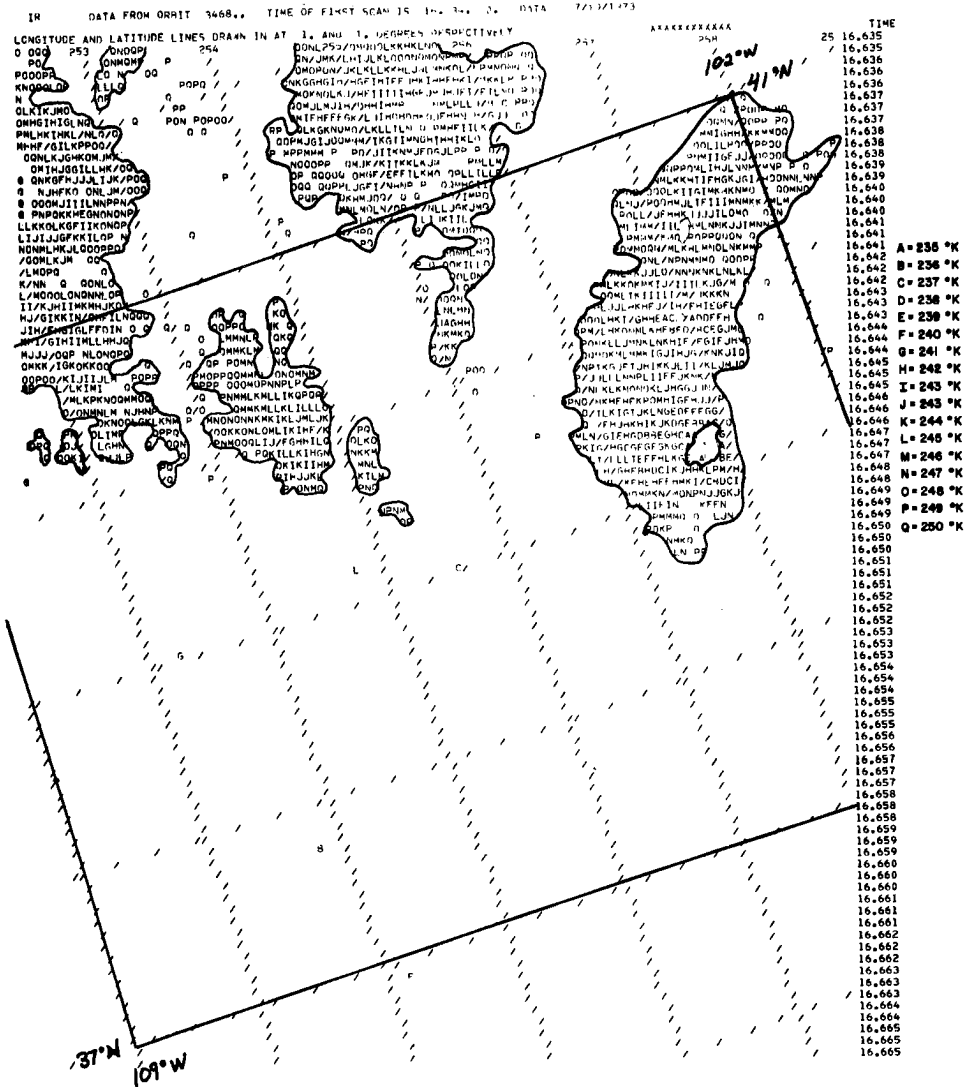


Figure 13 High Resolution (IR) output where only the higher type clouds have been depicted. Data displayed in this way can help define the areal extent of the high clouds as well as pin-point their location.

with what radar picked up at 1140 MDT. Thus the satellite data, in digital form, along with sounding data can identify, over a large area, cloud heights and augment radar data. This helps define areas where possible heavy rain will occur. On this day, Grover, Colorado and Cheyenne, Wyoming, did record 3.00 inches of rain.

This one example also shows that cirrus clouds can be identified by the IR temperatures as well as contrasting the visible and IR pictures to see if low albedoes occur with cold temperature. Thus it is possible to identify cirrus clouds in the computer which would be beneficial in another area of application which concerns monitoring the downwind effects of seeding in the NHRE area. Watching the day-to-day cirrus blow-off from thunderstorms and relating this to seed or no-seed days it should be possible to relate seeding to cirrus outflow and thus determine if more cirrus is produced and whether it affects convection downwind of the seed area (Brier and Grant, 1973).

3) As a forecast aid to predicting heavy snow along the front range of the Rocky Mountains.

This application would follow along the same lines as the description above except that we will be discussing snowfall. As can be seen by Fig. 14 there is a general upslope cloudiness extending over Colorado, New Mexico, Kansas and parts of Nebraska, Texas and Oklahoma. Again there are two levels of clouds; one lower upslope cloudiness - light precipitation, another deck with much higher tops (i.e., northern Colorado) where precipitation would be heavier. Again, the digital data provides cloud tops, locations and areal extents of the heavier type precipitation areas which could be used as an aid in forecasting. On this day parts of Fort Collins, Colorado, 60 mi. north of Denver received 3 inches of snow

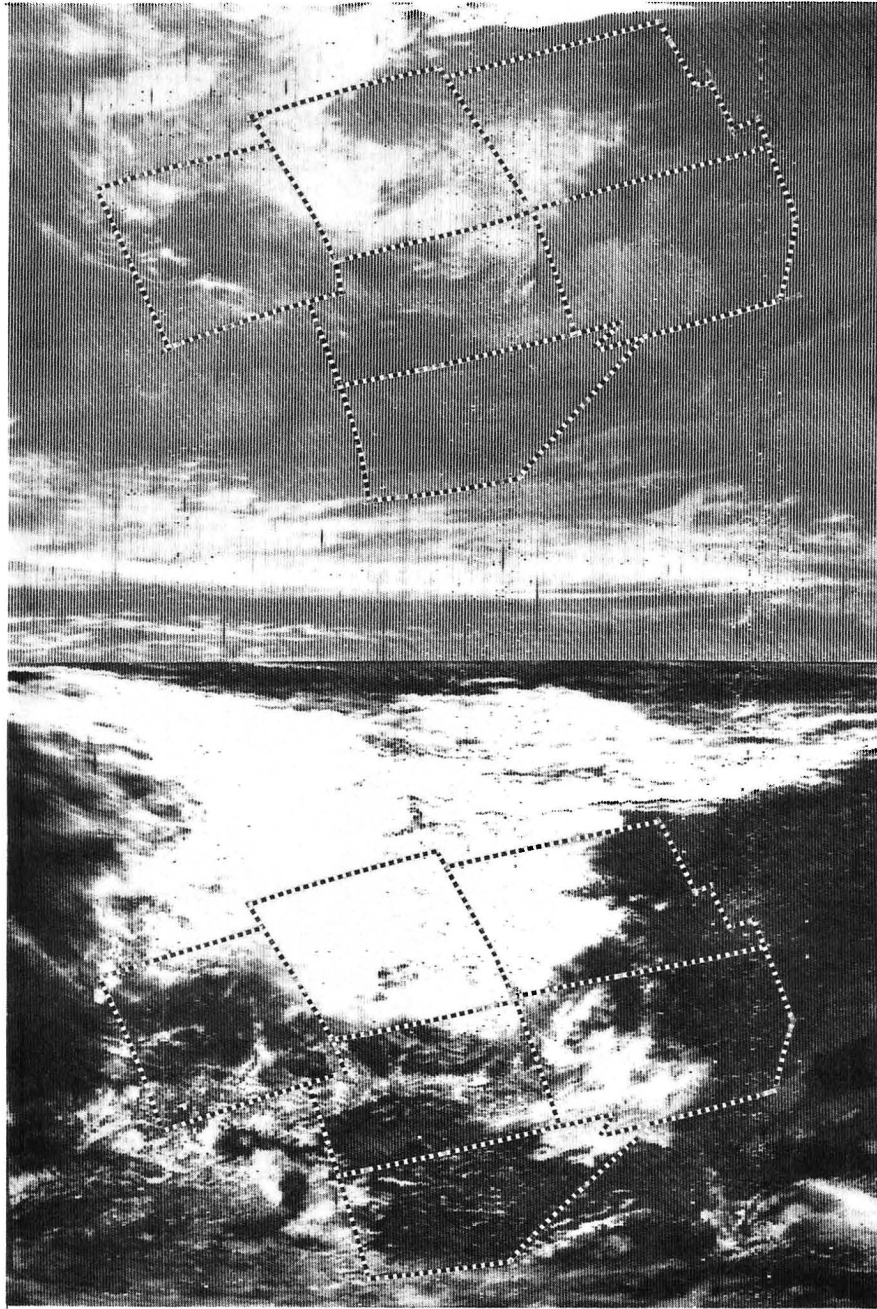


Figure 14 Visible (left) and IR (right) NOAA SR data for March 10, 1974 showing an upslope snowstorm system over eastern Colorado and northern New Mexico. Note contrast between the visible and IR data.

while Denver received only 1.5 inches. The high resolution IR output of Fig. 15 shows the higher clouds outside the black borders which would be the areas to watch for heavy snow.

These three areas discussed are only a few of the possible ways in which digitized satellite data could be used. Also the way in which the digital data is handled is infinite. The important point to remember is that it is possible to obtain this digital data at a relatively low cost.

4.0 SUMMARY

The fourth advance in usefulness of the direct readout VHF meteorological satellite data has been reported. With the addition of the "discrimination box", which is described in detail in this paper, a mini-computer (with a minimum of 16k core) and an A-D converter, any APT station has the capability of obtaining the described quantitative data. The programs described in this paper are only one approach to display and analysis of the digitized SR data. Once the data is in the form of reflectance or blackbody temperature, the mode of display and analysis is arbitrary. Here at Colorado State University we are working on a method to display the digital data in visual form on a television screen by use of a scan converter and mini-computer.

Several applications of the digital data have been described. It has been shown that many field projects such as in weather modification would benefit by the use of this data. Also small research groups or forecasting units that are out of reach of the normal stream of meteorological data (i.e., fax maps, teletype) could make very important use of the quantized data especially in local storm problems. The cost of this

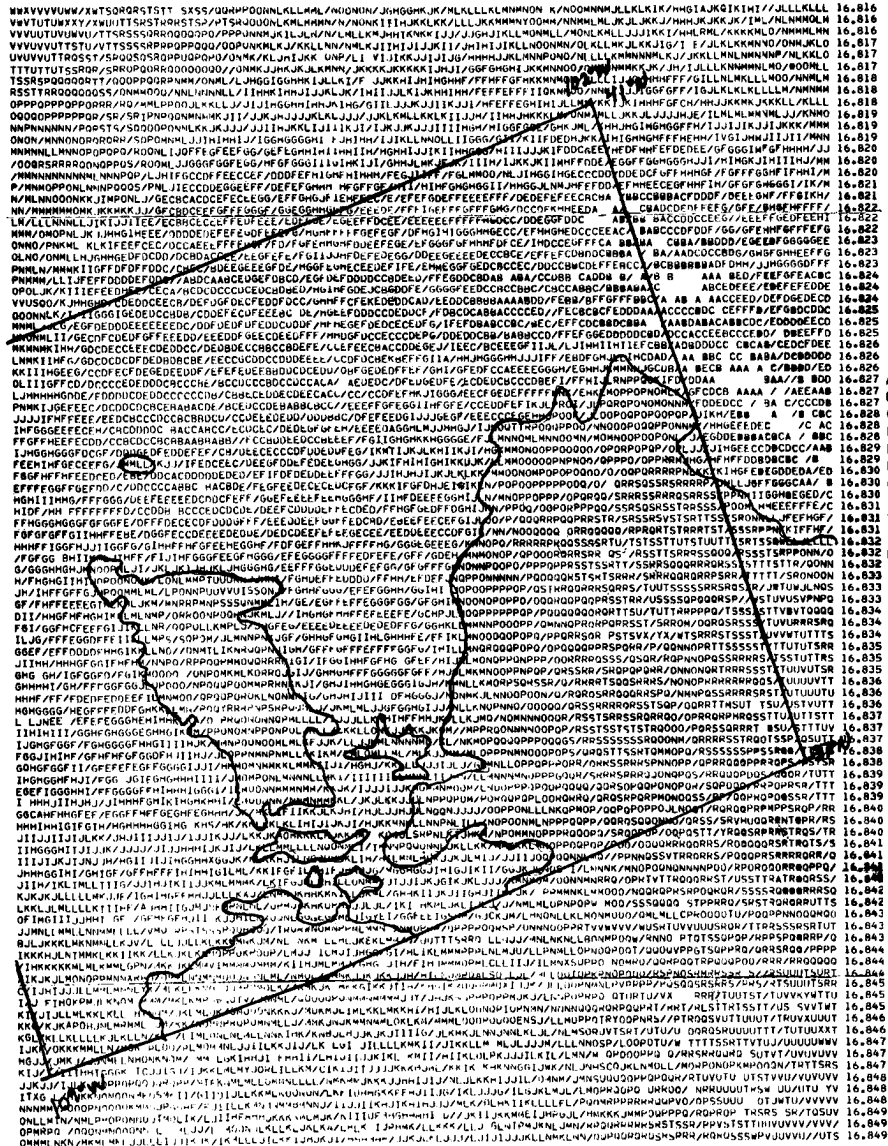


Figure 15 High resolution (IR) output for March 10, 1974 where areas within the black line have temperatures above 252°K. Those colder than 252°K are areas where the heavier precipitation would be most likely to occur.

system should not be prohibitive and in this lies the real fourth advance in the use of direct readout data.

5.0 REFERENCES

- Brier, G. W. and L. O. Grant, 1973: An evaluation of the extended area effects problem as related to the National Hail Research Experiment. Interim Report, Contract No. NCAR 32-72.
- Grant, L. O. and R. E. Elliott, 1974: The cloud-seeding temperature window. J. Appl. Meteor., 13, 3, 355-363.
- Madden, R., H. Miller, M. Polifka and T. Vonder Haar, 1972: Computer programs for direct read-out satellite data use. Tech. Report, Dept. of Atmospheric Science, Colorado State University, Fort Collins.
- Madden, R. A. and C. J. Parsons, 1973: A technique for real-time, quantitative display of APT scanning radiometer data. J. Appl. Meteor., 12, 2, 381-385.
- Miller, H. J. and T. H. Vonder Haar, 1972: Real-time direct read-out satellite support to meteorological research programs and forecasting units. Atmospheric Science Paper No. 181, Colorado State Univ., Fort Collins.
- National Environmental Satellite Center, ESSA Direct transmission user's guide. U.S. Dept. of Commerce, Wash. D. C. (1969).
- Schwalb, A., 1972: Modified version of the improved TIROS operational satellite (ITOS-D-G). NOAA Tech. Memorandum NESS 35. U.S. Dept. of Commerce publication.
- Sikula, G. J. and T. H. Vonder Haar, 1973: Very short range local area weather forecasting using measurements from geosynchronous meteorological satellite. Arch. Met. Geoph. Biokl., Ser. A., 22, 227-256.
- Vermillion, C. H., 1969: Weather satellite picture receiving stations. NASA Special Publications 5080.
- Vonder Haar, T. H. and D. W. Reynolds, 1974: Bi-spectral method for inferring cloud amount and cloud-top temperature using satellite data. Presented at Sixth Conf. on Aerospace and Aeronautical Meteor. of the AMS. Nov. 12-14, El Paso, Texas.
- Vonder Haar, T. H., 1970: Application of simultaneous infrared radiation measurements and cloud photographs from satellites. J. Appl. Meteor., 9, 6, 955-958.

6.0 ACKNOWLEDGEMENTS

We would like to thank Ms. Lyn Koch for the typing of this manuscript and Ms. Charline Polifka for her expertise in programming. We would also like to thank Ms. Karla Garretson for the drafting provided.

This research has been supported jointly by the Atmospheric Science Section, National Science Foundation under Grant GA-31588 and by the Atmospheric and Hydrospheric Applications Division, Goddard Space Flight Center, NASA, under Grant NSG 5011.

APPENDIX 1
Operation of the Discriminator Box

The satellite picture, which has previously been recorded, enters the unit at J1. The signal is taken from the recorder at the recorder preamplifier to avoid the distortion present in the power amplifier. The input buffer stage amplifies the tape signal from its 0.1 volt level to approximately 5 volts peak to peak. The gain of this stage is adjustable from 0 to 100 via R2. Capacitor C1 serves to block any dc which may be present in the recorder output. A test point is provided at the output of this stage for testing.

Since the picture information at this stage consists of an amplitude modulated 2.4 kHz carrier the next processing step is to begin demodulating the information by full wave rectification of the carrier. Ordinary semiconductor diodes could be used for this purpose. But these devices are essentially nonlinear and have a limited dynamic range. The addition of two operational amplifiers, however, allows us to place the diodes inside the feedback loop of the amplifier so that the nonlinearities are reduced to an insignificant amount. Looking at A2 (see Figure 16) we see that it is configured as a unity gain inverting amplifier with two feedback loops, D1-R7 and D2-R10. For negative inputs to A2 the loop is closed through D1-R7 and for positive signals through D2-R10. Thus for signals less than zero the voltage at point (a) will equal $-V_{in}$, while it will be zero for any positive input. Thus A2 acts as an ideal half wave rectifier. R11 is adjusted so that this transition occurs precisely at the zero crossing. Full wave rectification is achieved by adding the original signal and the half wave rectified signal in amplifier A3. A3 has two inputs R12 and R9.

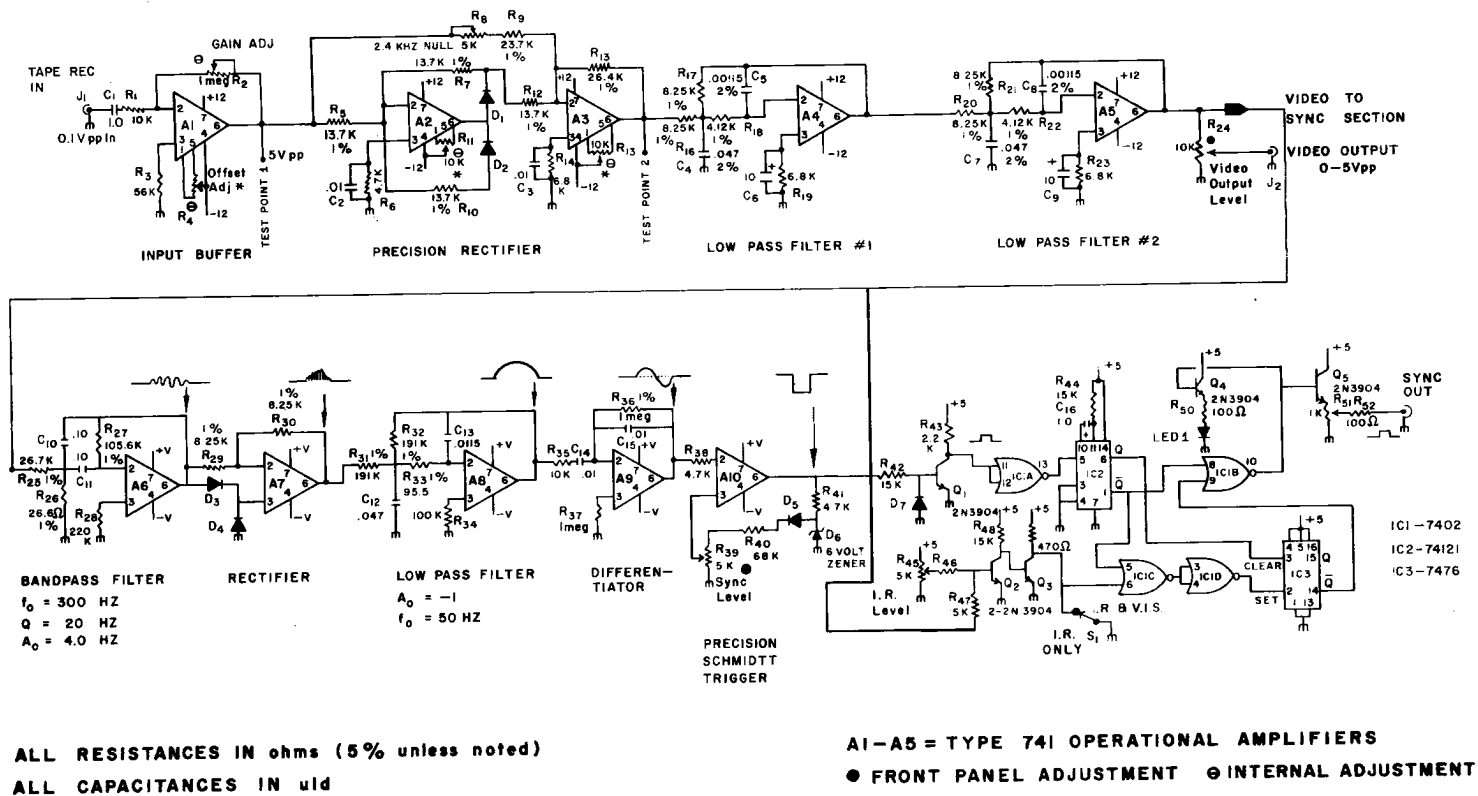


Figure 16 Schematic electrical diagram of the "Discriminator Box" used in the digitizing of the NOAA SR data.

The gain through R12 is twice that through R9. Thus during positive cycles, when A2 is not providing any signal, the output of A3 consists of only the inverted original signal. During the negative cycles A2 provides a signal offsetting the signal through R9 and the output of A3 is the noninverted original signal. R8 is provided so that the gain through R9 is exactly 0.50 times the gain through R12. When R8 is properly adjusted the amount of 2.4 kHz carrier in the rectified signal is at a minimum.

The picture information now consists of a waveform whose average amplitude corresponds to the transmitted data value and which fluctuates at a rate of 4.8 kHz. The purpose of the two low pass filters is to remove these fluctuations so that the average video level is developed. Since these filters are identical we will only describe one in detail. These filters have the configuration of a multiple feedback low pass filter. Component values have been chosen to provide a -3db point of 1.6 kHz and a roll off of 40 db/decade beyond this. Gain below the cutoff point is unity. The combination of the two filters provides 80 db/decade roll off with a -3 db point of approximately 1.0 kHz. Table I shows the measured response of these two filters in combination as a function of frequency. One can see that only 0.4% of the 4.8 kHz fluctuations pass through the filter. This amounts to about 20 mv in actual operation. One might question the advisability of such elaborate filtering. It is desirable to keep the maximum possible picture detail throughout the system. This requires a wide video bandwidth which is in conflict with maximum carrier suppression. The use of active filters with their attendant sharp cutoff allows both wide bandwidth in the video bassband and good ripple suppression. For example, if a simple RC filter were used and the ripple level

made the same as the unit now has (0.4%), then the video bandwidth would be only 150 hz, which would result in a considerable loss of picture detail.

The desired analog signal has now been recovered from the satellite signal. While it would be possible to randomly digitize this information and then locate the various picture elements by a software search, it is much more efficient to synchronize the digitizing process to the data stream by a hardware approach. This assures that the data is always digitized in the same order for each line in the picture. The following is a description of the hardware used to implement this synchronization.

The recovered video is sent to A6 which is configured into a band-pass filter. This filter has a Q factor of 20 and a midband gain of -4.0 and is centered at 300 Hz. The satellite signal carries synchronization in the form of seven cycles of a 300 Hz square wave. The bandpass filter responds to any 300 Hz component in the picture video, but the synchronization burst is by far the dominant feature. Because of the narrow bandwidth of the filter, about 15 Hz, the filters output begins to build as each cycle in the burst occurs. After the seventh cycle, at which time the filters output is at its peak, the filter "rings down" at 300 Hz for about another 10 cycles. Thus the end of the synch burst and the peak of the bankpass output occur simultaneously. Because of the narrow bandwidth of the filter, noise has very little effect on its output.

Amplifier A7 operates as a fullwave recitifier for the bandpass filters output. Fullwave rectification is used to double the frequency of the ripple component to 500 Hz and to detect the average envelope of the filters output. Amplifier A8 acts as a low pass filter with an upper cutoff of 50 Hz, a gain of -1.0, and a slope of -40 db/decade

above cutoff. It removes the ripple components from the detected bandpass output. The output of this filter consists of the envelope of the bandpass filter's output.

To locate the peak in this envelope we first differentiate the signal in A9. A9 acts as a stopped differentiator in that its high frequency response is limited by R35 and C15. This makes the differentiator less susceptible to high frequency noise. Otherwise it performs as a classical differentiator. A10 is used as a Schmidt trigger with one adjustable trip point and zero for the other trip point. In operation the output of A10 is normally at +15 volts. R41 and D6 regulate this positive output to 6.0 volts. D5 couples this voltage into the voltage divider R40 and R39. R39 is adjusted to provide a desired level at the non-inverting input to A10. When the output from A9 exceeds this level the output of A10 changes from +15 to -15 volts. D5 is now reverse biased and the voltage across R39 falls to zero. Correspondingly, the input to pin 3 of A10 falls to zero. The Schmidt trigger will remain in this state until the output of A9 falls through zero. Since the zero crossing of A9 corresponds to the peak of the bandpass envelope it corresponds to the end of the synch burst in the original picture video. Thus the -15 to +15 volt transition of A10 is the synchronization signal. In operation R39 is adjusted until the trigger is triggering randomly because of noise. Then it is set to the point where triggering does not quite occur on the actual synch signal. The control is then set halfway between these two extremes. Because of variations in the various tapes processed this control is made accessible from the front panel.

Q1 and IC1A act as a level shifter to change the output from A10 to a TTL compatible signal. IC2 is a one-shot multivibrator which provides a uniform trigger pulse, triggering on the rising edge of A10's output. The remaining circuitry is used to separate the IR lines from the visible lines. Q2 and Q3 act as a simple level comparator such that the output of Q3 is low if the video level is greater than the level set by R45. R45 is adjusted so that immediately after the synch burst Q3 will go low if the line is an IR line and will remain high if it is a visible lines. When the one-shot IC2 is fired flipflop IC3 can be set only if the line is an IR line; if not it remains in the cleared condition. If it is an IR line then IC1B is enabled and the synch pulse passes to the output stage. At the end of the one-shot timing period IC3 is cleared and IC1B is disabled. When it is desired to synchronize on both lines S1 is closed and Q3 is held low all the time. Q5 and Q4 act as emitter followers with Q5 driving the system output and Q4 driving a light emitting diode that is used as a visual synch indicator.

37
TABLE I
Composite Bandpass Characteristics

Frequency	Amplitude Relative
0.0	1.000
0.2	.993
0.4	.986
0.6	.947
0.8	.845
1.0k	.651
1.2k	.547
1.4k	.407
1.6k	.270
1.8k	.186
2.0k	.129
2.2	.0948
2.4	.0658
2.6	.0483
2.8	.0361
3.0	.0274
3.2	.0213
3.4	.0166
3.6	.0130
3.8	.0107
4.0	.0085
4.2	.0071
4.4	.0059
4.6	.0049
4.8	.0040
5.0	.0034

APPENDIX II

1.0 CALIBRATION DATA NEEDED TO CONVERT DIGITAL VOLTS TO SATELLITE VOLTS

NOAA-2 Step-Wedge Voltages (not known as function of Housing Temperature)

Step 1	Step 2	Step 3	Step 4	Step 5
1.2	2.4	3.6	4.8	6.0

NOAA-3 Step-Wedge Voltages (function of Housing Temperature)

T _{HOUSING}	Step 1	Step 2	Step 3	Step 4	Step 5
- 5°C	1.194	2.402	3.598	4.806	5.998
+ 5°C	1.195	2.402	3.599	4.806	5.996
+15°C	1.193	2.394	3.588	4.801	5.996
+35°C	1.194	2.399	3.589	4.804	5.988
+40°C	1.192	2.396	3.585	4.795	5.990
Room Temp.	1.199	2.401	3.591	4.802	5.987
Bench	1.200	2.402	3.591	4.798	5.994

Visible

T _{HOUSING}	Step 1	Step 2	Step 3	Step 4	Step 5
- 5°C	1.197	2.398	3.584	4.796	5.988
+ 5°C	1.198	2.395	3.586	4.795	5.986
+15°C	1.195	2.395	3.584	4.794	5.986
+35°C	1.195	2.399	3.590	4.793	5.985
+40°C	1.193	2.399	3.591	4.793	5.987
Room Temp.	1.197	2.398	3.587	4.793	5.982
Bench	1.192	2.393	3.584	4.795	5.988

It is these above values which are compared to the digital volts to obtain the linearized equation to convert from digital volts to satellite volts.

2.0 CALIBRATION DATA NEEDED TO CONVERT FROM SATELLITE VOLTS TO FOOT-LAMBERTS OR BLACKBODY TEMPERATURE

IR Temperature versus Volts for Noaa-2
4th Degree Polynomial

		x = volts
T_{HOUSING}		y = temperature
+15.0	$y = .1331098E+3x^4 - .1069548E+3x^3 - .3322545E+2x^2 - .5582265E+1x - .3511072E+0$	
+25.0	$y = .1338333E+3x^4 - .1050560E+3x^3 - .3195017E+2x^2 - .5330614E+1x - .3344988E+0$	
+27.5	$y = .1329672E+3x^4 - .1073187E+3x^3 - .3312039E+2x^2 - .5584758E+1x - .3537296E+0$	
+30.0	$y = .1329684E+3x^4 - .1075822E+3x^3 - .3310725E+2x^2 - .5556753E+1x - .3499417E+0$	
+32.5	$y = .1323005E+3x^4 - .1092760E+3x^3 - .3378705E+2x^2 - .5653134E+1x - .3537296E+0$	
+35.0	$y = .1316111E+3x^4 - .1110111E+3x^3 - .345671E+2x^2 - .5788526E+1x - .3624709E+0$	
+37.5	$y = .1313321E+3x^4 - .1113066E+3x^3 - .3441902E+2x^2 - .5764213E+1x - .3615967E+0$	
+40.0	$y = .1316162E+3x^4 - .1103458E+3x^3 - .3361286E+2x^2 - .5601917E+1x - .3519814E+0$	

NOAA-3

4th Degree Polynomial

T_{HOUSING}	
- 5.0	$y = .1385819E+3x^4 - .1028811E+3x^3 - .3182521E+2x^2 - .5457140E+1x - .3523499E+0$
+ 5.0	$y = .1380794E+3x^4 - .1018659E+3x^3 - .3113261E+2x^2 - .5278487E+1x - .3372950E+0$
+15.0	$y = .1387238E+3x^4 - .1011301E+3x^3 - .3070094E+2x^2 - .5183641E+1x - .3303776E+0$
+25.0	$y = .1386811E+3x^4 - .1023954E+3x^3 - .3183618E+2x^2 - .5540196E+1x - .3639028E+0$
+35.0	$y = .1405100E+3x^4 - .1018974E+3x^3 - .3142833E+2x^2 - .5465066E+1x - .3607309E+0$
+40.0	$y = .1382594E+3x^4 - .1079273E+3x^3 - .3501205E+2x^2 - .6394881E+1x - .4429862E+0$